Published in final edited form as:
Curr Eye Res. 2013 December ; 38(12): 1229–1234. doi:10.3109/02713683.2013.815219.

Fundus Camera Guided Photoacoustic Ophthalmoscopy

Tan Liu[1,*], **Hao Li**[1,*], **Wei Song**[1,2], **Shuliang Jiao**[3], and **Hao F. Zhang**[1,4]

[1]Department of Biomedical Engineering, Northwestern University, Evanston, IL, USA

[2]Department of Physics, Harbin Institute of Technology, Harbin, Heilongjiang, P.R. China

[3]Department of Biomedical Engineering, Florida International University, Miami, FL, USA

[4]Department of Ophthalmology, Northwestern University, Chicago, IL, USA

Abstract

Purpose—To demonstrate the feasibility of fundus camera guided photoacoustic ophthalmoscopy (PAOM) system and its multimodal imaging capabilities.

Methods—We integrated PAOM and a fundus camera consisting of a white-light illuminator and a high-sensitivity, high-speed CCD. The fundus camera captures both retinal anatomy and PAOM illumination at the same time to provide a real-time feedback when we position the PAOM illuminating light. We applied the integrated system to image rat eyes *in vivo* and used full-spectrum, visible (VIS), and near infrared (NIR) illuminations in fundus photography.

Results—Both albino and pigmented rat eyes were imaged *in vivo*. During alignment, different trajectories of PAOM laser scanning were successfully visualized by the fundus camera, which reduced the PAOM alignment time from several minutes to 30 s. In albino eyes, in addition to retinal vessels, main choroidal vessels were observed using VIS-illumination, which is similar to PAOM images. In pigmented eyes, the radial striations of retinal nerve fiber layer were visualized by fundus photography using full-spectrum illumination; meanwhile, PAOM imaged both retinal vessels and the retinal pigmented epithelium melanin distribution.

Conclusions—The results demonstrated that PAOM can be well-integrated with fundus camera without affecting its functionality. The fundus camera guidance is faster and easier comparing with our previous work. The integrated system also set the stage for the next-step verification between oximetry methods based on PAOM and fundus photography.

Keywords

Fundus camera; multimodal imaging; photoacoustic ophthalmoscopy; retina; retinal imaging

Correspondence: Hao F. Zhang, Northwestern University, Department of Biomedical Engineering, Evanston 60208, USA. hfzhang@northwestern.edu.
*Authors contributed equally to this work.

DECLARATION OF INTEREST
The authors report no conflicts of interest.

INTRODUCTION

Photoacoustic ophthalmoscopy (PAOM) is a recently-developed high-resolution, noninvasive *in vivo* retinal imaging technology.[1,2] It introduces a low-energy, pulsed laser beam focused on the retina. Optical absorbing chromophores such as hemoglobin and melanin at the focal point absorb the optical energy, which generates ultrasound waves. By scanning laser light and detect the time-resolved ultrasonic signals from different retina position, we can obtain a map of retinal structure in three dimensions with high spatial resolution along both axial and lateral directions. In comparison, fundus photography and scanning laser ophthalmoscope (SLO) have no or only poor axial resolution, which make them only two-dimensional imaging modalities.

The most unique feature of PAOM is its source of imaging contrast. Different from most of the existing retina imaging techniques including fundus photography, SLO, and optical coherence tomography (OCT) that rely on back-reflected light, PAOM relies on the absorbed light for imaging. Although optical absorption properties of the retina are now being evaluated indirectly using optical reflection based technologies, these methods often requires over-simplified mathematical models of photon transport in the retina.[3] Moreover, by using different excitation light wavelengths, PAOM has the potential to accurately obtain absorption spectra of different retinal layers and provides physiologically related information in the eye that no other existing ophthalmic imaging technologies can. For example, the differences in the optical absorption spectra of oxygenated and deoxygenated hemoglobin offer PAOM an opportunity to measure hemoglobin oxygen saturation (sO_2) in retinal vessels, which is believed to be a missing key parameter in order to better understand and diagnose early-stage diabetic retinopathy.[4,5] Measuring the optical absorption information of the retinal pigment epithelium (RPE) may also provide information about RPE cell dysfunction, which is related to several blinding diseases including age-related macular degeneration (AMD).[6,7] Recently, high contrast *in vivo* imaging of the retinal vessels,[1] choroidal vascular network,[8] and RPE melanin[5,9] were demonstrated in rodents.

Prior to imaging, PAOM usually needs help from an additional imaging modality for alignment and identifying region-of-interest (ROI).[1] Based on laser-scanning optical-resolution photoacoustic microscopy, PAOM relies on good optical focus to provide both high spatial resolution and high signal-to-noise ratio (SNR); hence, optical alignment should be done before data acquisition.[1,2] PAOM currently uses visible light for imaging aiming at the strong optical absorption of hemoglobin and melanin. Repetitive illumination during alignment and searching for ROI can be uncomfortable for the imaging subject and can potentially raise safety concerns.[10] As a result, a high-speed imaging modality, preferably working within near-infrared (NIR) spectral range, is preferred to guide PAOM optical alignment. Moreover, adding an additional imaging modality will provide capabilities to capture multiple optical contrasts for more comprehensive retinal imaging.[11]

Previously, we integrated a spectral-domain optical coherence tomography (SD-OCT, working at 850nm center wavelength) in confocal with PAOM.[1,5,7,8,10] When we finished aligning SD-OCT optics and identifying its imaging ROI, we considered that PAOM optical alignment was also achieved. Normally it took 5–10 min to finish the alignment.

Fundus camera provides real-time *en face* view of the retina and has been widely used to provide video guidance in commercial SD-OCT systems.[12] If fundus camera can be integrated with PAOM, the optical alignment will be much faster and identifying ROI will be much easier because PAOM optical illumination can also be visualized by fundus camera in real time. Moreover, since Monte Carlo simulation has shown that PAOM retinal oximetry is more accurate than existing fundus photography-based oximetry,[3] integrating a fundus camera with PAOM provides a platform to validate the simulation results and, potentially, to develop methodologies to improve the existing fundus photography-based retinal oximetry.

In this report, we demonstrated the feasibility to integrate a fundus camera with PAOM. We applied the integrated system to image both albino and pigmented rat eyes *in vivo*. We also compared fundus photography results using optical illuminations at different spectral ranges.

METHODS

Experimental System

A schematic of the imaging system designed and optimized for rat eyes is shown in Figure 1. A 532-nm pulsed laser (Nd:YAG laser, SPOT-10-100, Elforlight Ltd, UK; output wavelength 1064 nm; pulse duration: 2 ns; BBO crystal for second harmonic frequency generation; CasTech, San Jose, CA) was used as the illumination light source for PAOM. The PAOM laser (green path) was scanned by an x–y galvanometer (QS-7, Nutfield Technology) and delivered to the posterior segment of the eye after passing through a relay lens L5 (f = 150mm) and an objective lens OBJ1 (f = 30mm, VIS-NIR AR coated). The final laser pulse energy on the cornea is 60 nJ, which is considered eye-safe.[9]

The induced PA waves were detected by a custom-built unfocused needle ultrasonic transducer (central frequency 35 MHz; bandwidth: 50%; active element size: 0.5 × 0.5mm^2). The ultrasonic transducer was gently attached to the eye lid (close to the canthus) coupled by a thin layer of medical-grade ultrasound gel. The detected PA signals were amplified by 69 dB, digitized and recorded by a computer. To avoid jittering associated with the excitation laser, PAOM data acquisition was triggered by the laser pulse through a photodiode (DET10A, Thorlabs). PAOM worked at a 24-kHz A-line rate. To acquire a full-field PAOM fundus image, the scan angle was 20°, which covered an area of approximately 2.1 × 2.1mm^2 on the rat retina.

The light path of the fundus camera is colored in red in Figure 1(a).[13–15] A tungsten halogen bulb was used as the light source. An optional filter was placed in front of the bulb for illumination spectrum selection. Light coming out of the bulb first passed through an annular stop to generate a ring illumination; then the beam was reduced in size and was imaged onto the cornea by lenses L1 (f = 100 mm), L2 (f = 40 nm) and L3 (f = 150 mm). The fundus illuminating light was combined with the detecting path and the PAOM illumination path by SP1 and SP2 (EBS1, Thorlabs). The maximum power of the fundus illumination light on the cornea was 0.8 mW. The backscattered light from retina passed through L4 (f = 100mm, Thorlabs) and OBJ2 (f = 90 mm), and was detected by a scientific

monochrome CCD camera (Pixelfly qe, 1392 × 1040 pixels, PCO AG; 150 ms integration time; free-running mode).

The spectra of the three different illuminations used in fundus photography are shown in Figure 1(b). No filter was applied for the full-spectrum illumination; a visible band-pass filter (FGB37M, Thorlabs) and a NIR long-pass filter (FGL780M, Thorlabs) were used for VIS- and NIR-illumination in fundus photography.

As reported in our previous work,[1] PAOM has a lateral resolution of ~20 μm and the lateral resolution of the fundus camera is estimated as 10–20 μm.[16] The axial resolution of PAOM is 23 μm, which is determined by the ultrasonic bandwidth; the fundus camera has only poor axial resolution.

Animal Preparations

Wild-type albino and pigmented rats (250 g Sprague Dawley and Long Evans rats; Charles River Laboratories) were used for *in vivo* imaging. The rats were anesthetized and kept motionless by a mixture of 1.5% isoflurane and oxygen at a flow rate of 1.5 l/min. During experiments, the animals were placed in a homemade animal holder. We added one drop of 0.5% Tetracaine Hydrochloride ophthalmic solution to the eyes for local anesthesia and one drop of 1% Tropicamide ophthalmic solution to dilate the pupils. Artificial tears were applied every other minute to prevent cornea dehydration. All the experiments were performed in compliance with the ARVO Statement for the Use of Animals in Ophthalmic and Vision Research, and were approved by the Animal Care and Use Committee of Northwestern University.

RESULTS AND DISCUSSIONS

The Fundus Camera Guided PAOM Imaging Positioning

A snapshot of the fundus camera real-time video around the optic disc (wild-type Long Evans rat) with line scan and circular scan patterns of PAOM illuminations are shown in Figure 2(a) and (b), respectively. We can clearly observe the PAOM scanning trajectories and retinal anatomy from the fundus camera video simultaneously.

Using the current system, positioning the optic disc to the center of field-of-view (FOV) took less than 30 s, which was much faster than our previous work.[1] Due to observation of the PAOM laser focus in real time, we were able to quickly and precisely select a ROI for PAOM. Such a simplified operation can be very beneficial to shorten the whole imaging procedure and prepare PAOM well for clinical applications.

PAOM and Fundus Camera Imaging in Albino Eyes

Figure 3 shows the *in vivo* fundus camera and PAOM images from an albino rat eye. A full-spectrum-illumination fundus camera image is shown in Figure 3(a). All the main retinal vessels can be observed, however, with limited contrast. The backscattering signal intensities are low along the center-line of the blood vessels and are much higher in regions outside the blood vessels due less optical attenuation by blood. A few large chorodial vessels

are vaguely observed. The low contrast in Figure 3(a) is mainly caused by the strong optical reflections from both vessels and avascular regions under the full spectrum illumination.

The VIS-illumination fundus image is shown in Figure 3(b). Strong signals can only be observed from the regions outside the major blood vessels due to the strong optical absorption of blood within the VIS range.[17] Hence, the vascular network is visualized with negative contrast. Furthermore, due to the lack of melanin in the albino eye's RPE, light can reach the choroidal layer and resolve some choroidal vessels. A NIR-illumination fundus image is shown in Figure 3(c). The contrast of the vessels drops and only retinal vasculature can be vaguely visualized with low contrast, indicating a decrease in the blood absorption. The result is similar to what being previously reported.[18]

A PAOM image with a FOV corresponding to the region highlighted by the dashed-square in Figure 3(c) is shown in Figure 3(d). Compared with the VIS-illumination fundus image, where retinal vessels' axial information is missing, the PAOM imaging gives more spatial details due to its three-dimensional imaging capability. The PAOM also shows more details and clearly distinguishes the retinal vessels and choroidal vessels which are identical in the VIS-illumination fundus image.

PAOM and Fundus Camera Imaging in Pigmented Eyes

The retinal images of a wild-type Long Evans rat are shown in Figure 4. Figure 4(a) is the full-spectrum-illumination fundus image. Compared with Figure 3(a), the reflection from the regions without main vessels is lower due to the RPE melanin absorption and the radial striations of retinal nerve fiber layer (RNFL) are clearly observed.[16,19]

A VIS-illumination fundus image in the pigmented rat is shown in Figure 4(b), where no choroidal vessels can be observed because of the strong optical absorption by the RPE melanin. A NIR-illumination fundus image is shown in Figure 4(c). it is similar to the VIS-illuminated image except that reflection from the regions outside retinal vessels is stronger, which is possibly caused by less optical absorption by the RPE pigments. The PAOM fundus image is shown in Figure 4(d). Besides the clearly imaged retinal vessels, RPE is also imaged with high contrast with its PA signal amplitude comparable to that from the vessels. The uneven melanin distribution is also mapped accordingly by PA signal intensities from different locations in the RPE.

We believe the quality of the fundus camera image can be further improved. A mirror with a hollow center can be applied to introduce the illumination light to further reduce the specular reflection from corneal center.[19] High-quality achromatic lenses can be employed to reduce image aberration under different illumination wavelength.

More importantly, the integrated fundus camera and PAOM provides a platform to cross-verify results from each other to achieve accurate measurement of retinal sO_2. Using the integrated system, multispectral fundus photography and multispectral PAOM can be achieved on the same subject; thus, retinal oximetry using both methods can be compared side by side to verify conclusions from our Monte Carlo simulation.[12] Using cross-modality data, numerical compensations for fundus photography based oximetry[20–23] can be

compared with PAOM results and verified experimentally, which provides a foundation to develop computational methods to improve the accuracy of existing retinal oximetry.

CONCLUSION

In this work, we developed a fundus camera guided PAOM system and tested the system in both albino and pigmented rat eyes *in vivo*. To prepare for future retinal oximetry, we used different spectral illumination in fundus camera. The results show that the PAOM can be well-guided by fundus camera without affecting their respective functionalities. The alignment of PAOM became faster and easier than our previous work. This multimodal system has a potential impact on bringing PAOM closer to clinical settings and improving fundus-camera-based retinal oximetry by comparing with PAOM oximetry.

Acknowledgments

This work is supported in part by NSF grants CBET-1055379 (CAREER) and CBET-1066776, and NIH grants 1RC4EY021357, 1R01EY019951 and 1R24EY022883, and a pilot grant from the Illinois Society for the Presentation of Blindness. The authors alone are responsible for the content and writing of the paper.

REFERENCES

1. Jiao S, Jiang M, Hu J, Fawzi A, Zhou Q, Shung KK, et al. Photoacoustic ophthalmoscopy for in vivo retinal imaging. Opt Express. 2010; 18:3967–3972. [PubMed: 20389409]
2. Zhang HF, Puliafito CA, Jiao S. Photoacoustic ophthalmoscopy for *in vivo* retinal imaging: current status and prospects. Ophthalmic Surg Lasers Imaging. 2011; 42:S106–S115.
3. Liu W, Jiao S, Zhang HF. Accuracy of retinal oximetry: a Monte Carlo investigation. J Biomed Opt. 2013; 18:66003.
4. Wangsa-Wirawan ND, Linsenmeier RA. Retinal oxygen: fundamental and clinical aspects. Arch Ophthalmol. 2003; 121:547–557. [PubMed: 12695252]
5. Hardarson SH, Stefánsson E. Retinal oxygen saturation is altered in diabetic retinopathy. Br J Ophthalmol. 2012; 96:560–563. [PubMed: 22080478]
6. Zhang X, Zhang HF, Puliafito CA, Jiao S. Simultaneous in vivo imaging of melanin and lipofuscin in the retina with photoacoustic ophthalmoscopy and autofluorescence imaging. J Biomed Opt. 2011; 16:080504. [PubMed: 21895304]
7. Delori FC, Goger DG, Dorey CK. Age-related accumulation and spatial distribution of lipofuscin in RPE of normal subjects. Invest. Ophthalmol. Vis Sci. 2001; 42:1855–1866. [PubMed: 11431454]
8. Wei Q, Liu T, Jiao S, Zhang HF. Image chorioretinal vasculature in albino rats using photoacoustic ophthalmoscopy. J Mod Opt. 2011; 58:1997–2001.
9. Liu T, Wei Q, Song W, Burke JM, Jiao S, Zhang HF. Near-infrared light photoacoustic ophthalmoscopy. Biomed Opt Express. 2012; 3:792–799. [PubMed: 22574266]
10. Delori FC, Webb RH, Sliney DH. Maximum permissible exposures for ocular safety (ansi 2000), with emphasis on ophthalmic devices. J Opt Soc Am A Opt Image Sci Vis. 2007; 24:1250–1265. [PubMed: 17429471]
11. Song W, Wei Q, Liu T, Kuai D, Burke JM, Jiao S, Zhang HF. Integrating photoacoustic ophthalmoscopy with scanning laser ophthalmoscopy, optical coherence tomography, and fluorescein angiography for a multimodal retinal imaging platform. J Biomed Opt. 2012; 17:061206. [PubMed: 22734736]
12. Carl Zeiss Meditec, CIRRUS Family Datasheet. Available from: http://www.meditec.zeiss.com/C125679E00525939/ContainerTitel/CirrusOCT/$File/cirrus_family_flyer.pdf.
13. Ye H, Gao Z, Luo T, Huang Y. Optical configuration of fundus camera based on inner focusing manner. Chin Opt Lett. 2010; 8:689–692.

14. DeHoog E, Schwiegerling J. Optimal parameters for retinal illumination and imaging in fundus cameras. Appl Opt. 2008; 47:6769–6777. [PubMed: 19104528]
15. Link D, Strohmaier C, Seifert BU, Riemer T, Reitsamer HA, Haueisen J, Vilser W. Novel non-contact retina camera for the rat and its application to dynamic retinal vessel analysis. Biomed Opt Express. 2011; 2:3094–3108. [PubMed: 22076270]
16. Goatman KA. A reference standard for the measurement of macular oedema. Br J Ophthalmol. 2006; 90:1197–1202. [PubMed: 16929064]
17. Scott P. Optical Absorption of Hemoglobin. Available from: http://omlc.ogi.edu/spectra/hemoglobin/index.html.
18. Elsner AE, Burns SA, Weiter JJ, Delori FC. Infrared imaging of subretinal structures in the human ocular fundus. Vision Res. 1996; 36:191–205. [PubMed: 8746253]
19. Kawaguchi I, Higashide T, Ohkubo S, Takeda H, Sugiyama K. *In vivo* imaging and quantitative evaluation of the rat retinal nerve fiber layer using scanning laser ophthalmoscopy. Invest Ophthalmol Vis Sci. 2006; 47:2911–2916. [PubMed: 16799033]
20. Harris A, Dinn RB, Kagemann L, Rechtman LE. A review of methods for human retinal oximetry. Ophthalmic Surg Lasers Imaging. 2003; 34:152–164. [PubMed: 12665234]
21. Ramella-Roman JC, Mathews SA, Kandimalla H, Nabili A, Duncan DD, D'Anna SA, et al. Measurement of oxygen saturation in the retina with a spectroscopic sensitive multi aperture camera. Opt Express. 2008; 16:6170–6182. [PubMed: 18545319]
22. Hammer M, Vilser W, Riemer T, Schweitzer D. Retinal vessel oximetry-calibration, compensation for vessel diameter and fundus pigmentation, and reproducibility. J Biomed Opt. 2008; 13:054015. [PubMed: 19021395]
23. Hammer M, Leistritz S, Leistritz L, Schweitzer D. Light paths in retinal vessel oximetry. IEEE Trans Biomed Eng. 2001; 48:592–598. [PubMed: 11341533]

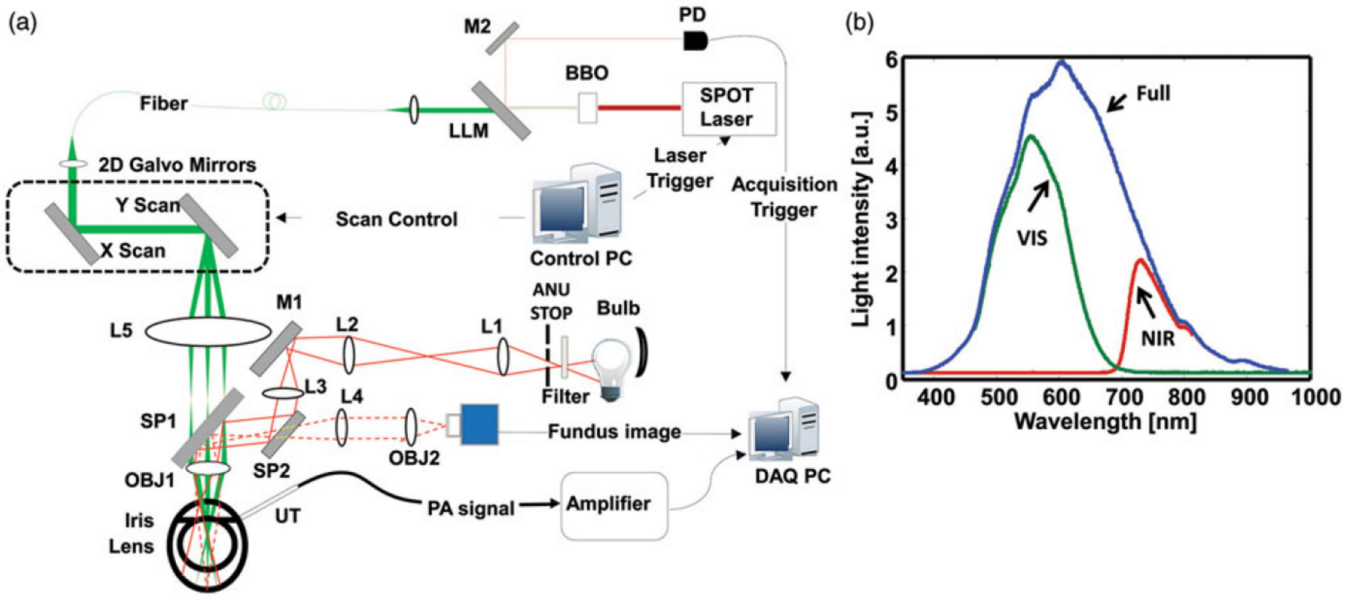

FIGURE 1.

The integrated fundus camera and PAOM. (a) Schematic of the imaging setup. PD: photodiode; DM: dichroic mirror; LLM: Laser Line Mirror; M1, M2: Mirror; UT: ultrasonic transducer; L1-L5: Lens; SP1, SP2, beam splitter; OBJ1, OBJ2: objective lens; ANU STOP: annulus stop; DAQ PC: data acquisition computer; (b) Different optical illumination spectrum used in fundus photography. Full spectrum is corresponding to the illumination without filter; VIS spectrum is achieved with 335–610nm filter; and NIR spectrum is achieved with 780-nm long pass filter.

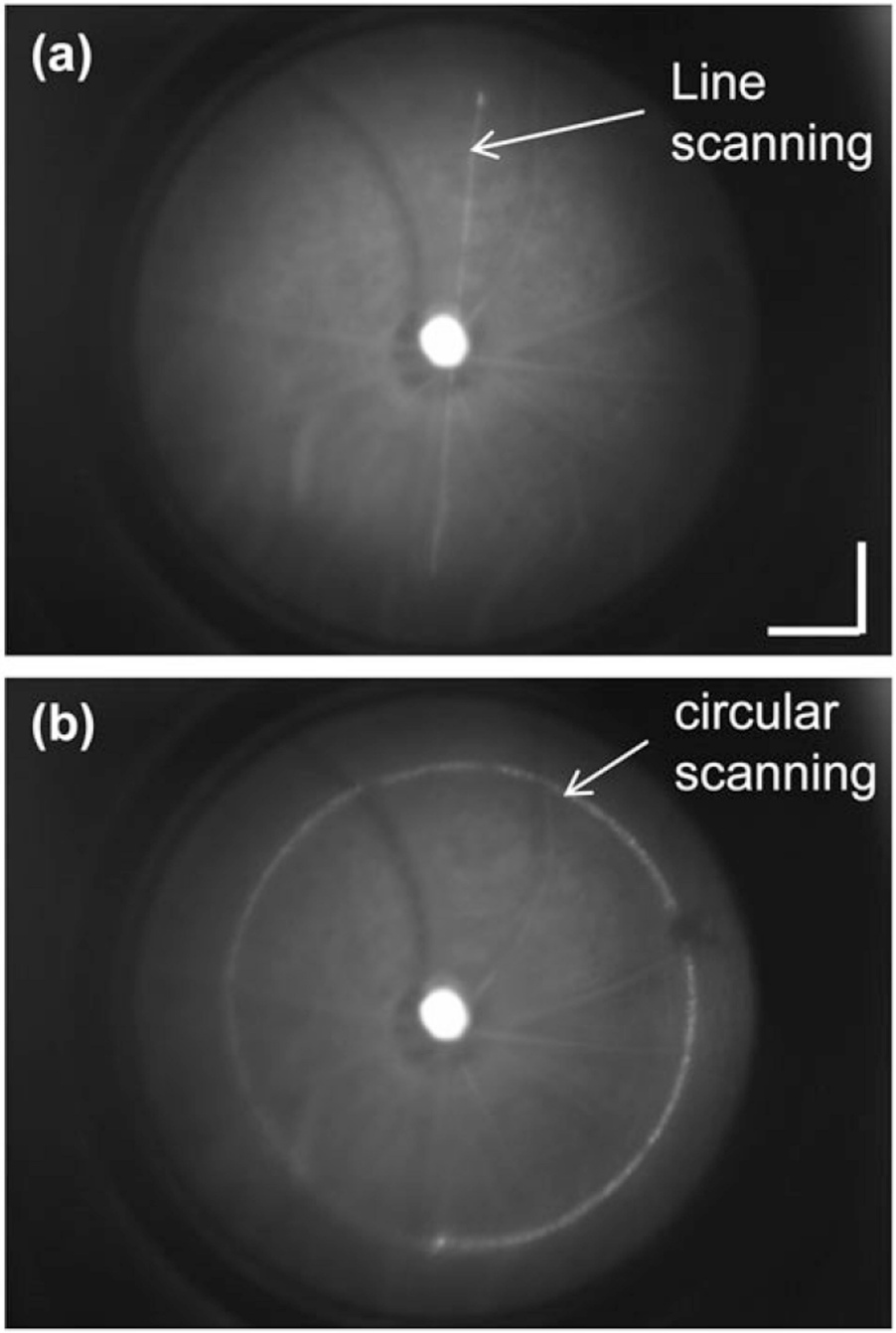

FIGURE 2.

Screen captures from real-time monitoring of PAOM laser scanning trajectories during alignment. (a) Radial line scan; (b) Circular scan. Bar: 500 μm.

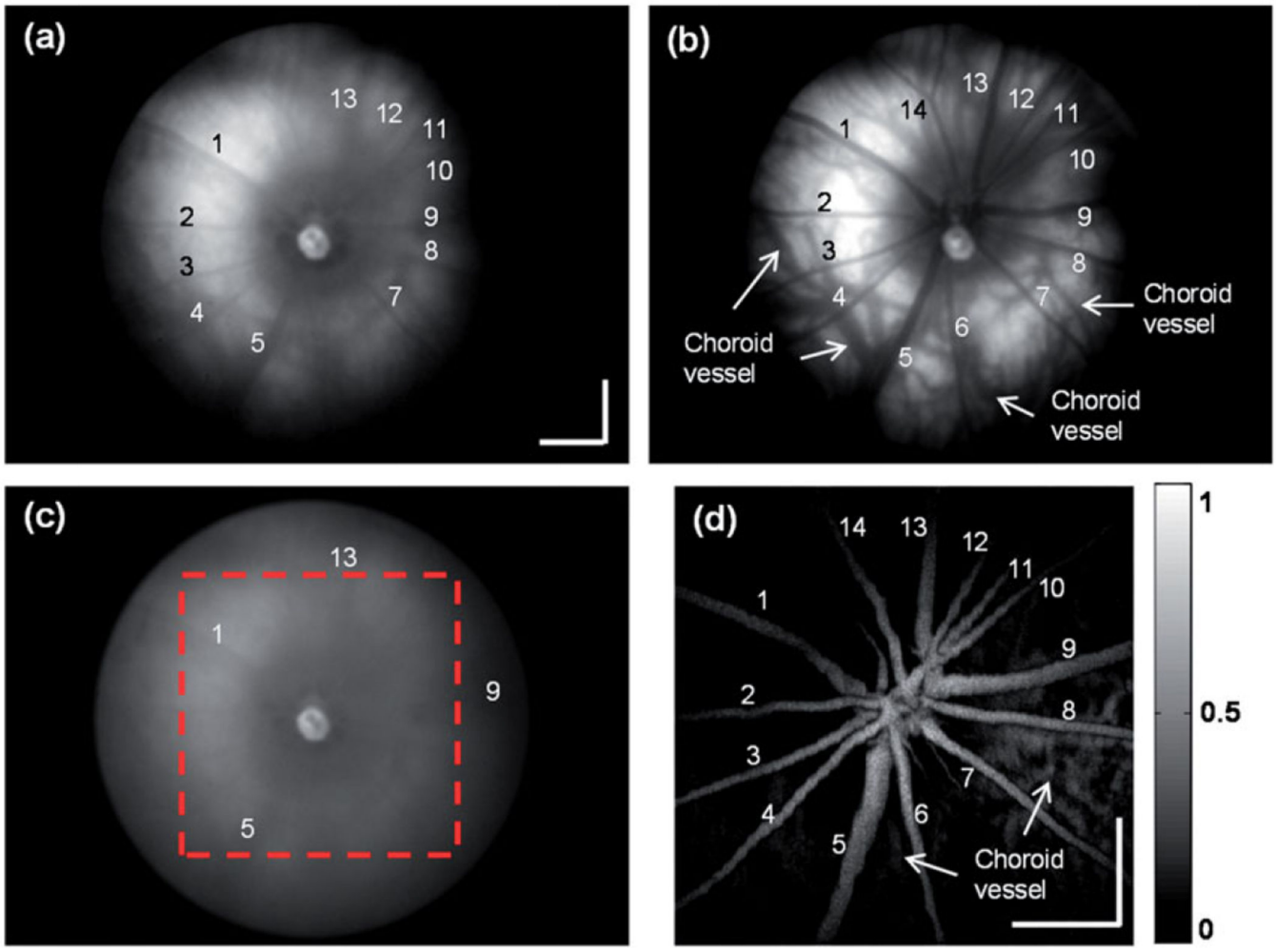

FIGURE 3.

In vivo images of an albino rat eye. (a) Full spectrum illumination fundus camera image; (b) VIS illumination fundus camera image; (c) NIR illumination fundus camera image; (d) PAOM fundus image within the dashed-square highlighted in panel c. As much as 14 major retinal vessels are labeled in both fundus camera and PAOM images. Bar: 500 μm.

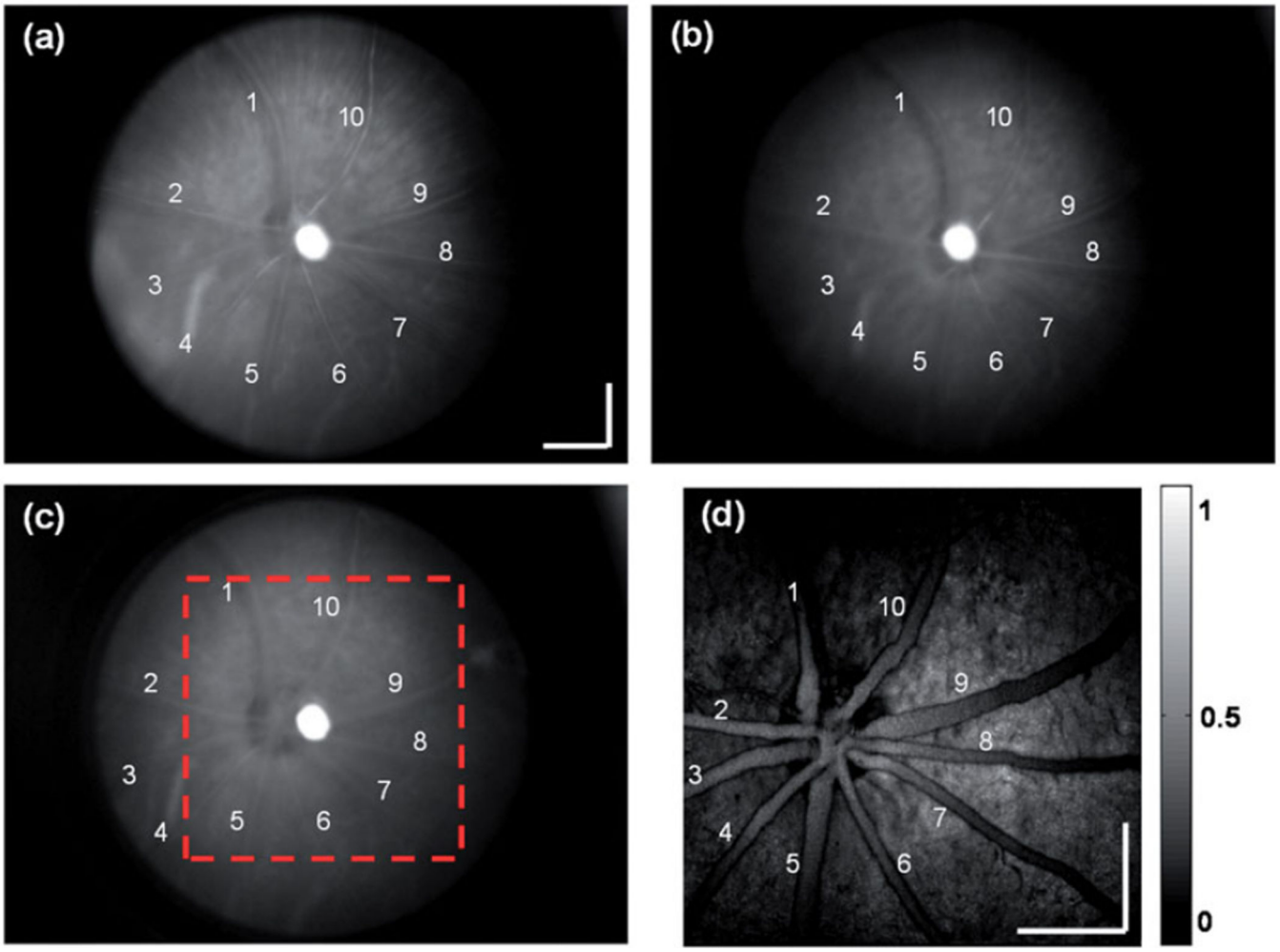

FIGURE 4.

In vivo images of a pigmented rat eye. (a) Full spectrum illumination fundus camera image; (b) VIS illumination fundus camera image; (c) NIR illumination fundus camera image; (d) PAOM fundus image within the dashed square highlighted in panel c. Ten major retinal vessels are labeled in both fundus camera and PAOM images. Bar: 500 μm.